Neural control of lipid metabolism and inflammation : implications for atherosclerosis

Kooijman, Sander

8

SPLENIC DENERVATION DOES NOT AGGRAVATE ATHEROSCLEROTIC LESION DEVELOPMENT IN APOE*3-LEIDEN.CETP TRANSGENIC MICE

Sander Kooijman
Illiana Meurs
Lianne van Beek
P. Padmini S.J. Khedoe
Annabel Giezekamp
Karin Pike-Overzet
Catthy Cailotto
Jan van der Vliet
Vannesa van Harmelen
Guy Boeckxstaens
Jimmy F.P. Berbée
Patrick C.N. Rensen

Am J Physiol Heart Circ Physiol (2015) 309: H646-54

Abstract

The brain plays a prominent role in the regulation of inflammation. Immune cells are under control of the so-called cholinergic anti-inflammatory reflex, mainly acting via autonomic innervation of the spleen. Activation of this reflex inhibits the secretion of pro-inflammatory cytokines and may reduce the development of atherosclerosis. Therefore, the aim of this study was to evaluate the effects of selective parasympathetic (Px) and sympathetic (Sx) denervation of the spleen on inflammatory status and atherosclerotic lesion development. Female APOE*3-Leiden.CETP mice, a well-established model for human-like lipid metabolism and atherosclerosis, were fed a cholesterol-containing Western-type diet for 4 weeks after which they were sub-divided into three groups receiving either splenic Px, splenic Sx or sham surgery. The mice were subsequently challenged with the same diet for an additional 15 weeks. Selective Px increased leukocyte counts (i.e. dendritic cells, B cells and T cells) in the spleen and increased gene expression of pro-inflammatory cytokines in the liver and peritoneal leukocytes as compared to Sx and sham surgery. Both Px and Sx increased circulating pro-inflammatory cytokines IL-1ß and IL-6. However, the increased pro-inflammatory status in denervated mice did not affect atherosclerotic lesion size or lesion composition. Predominantly selective Px of the spleen enhances the inflammatory status, which however does not aggravate diet-induced atherosclerotic lesion development.

Introduction

Atherosclerosis is a chronic inflammatory disease initiated by innate and adaptive immune responses to endogenously modified structures, in particular oxidized lipoproteins, within the arterial wall (1). The autonomic nervous system may enhance innate immune responses by sympathetic activity (2), while it suppresses inflammation via the vagus nerve, a mechanism termed the cholinergic anti-inflammatory pathway (3,4). In response to circulating pro-inflammatory cytokines afferent vagal nerves are directly activated. Subsequent efferent vagal activity results in the release of acetylcholine which activates the α7 nicotinic acetylcholine receptor (α7nAChR) on resident tissue macrophages and other immune cells, thereby inhibiting the production and release of pro-inflammatory cytokines (e.g. TNFα, IL-6, IL-1ß) (5). α7nAChR is integral to the cholinergic anti-inflammatory pathway, as vagus nerve stimulation fails to inhibit TNFα production in pharmacologically α7nAChR inhibited or α7nAChR-deficient mice (5,6). Recently, we demonstrated that hematopoietic α7nAChR deficiency in dyslipidemic mice enhances systemic inflammation as evidenced by increased leukocytes in the blood, lymph nodes, spleen and peritoneum (all by at least 2-fold) and increased gene expression of TNFα in peritoneal leukocytes and spleen (7).

As the spleen contains half of the body's monocyte population, it is not surprising that the cholinergic anti-inflammatory pathway acts mainly via the spleen. Indeed, Huston *et al.* (8) reported that vagus nerve stimulation fails to inhibit TNFα production in splenectomised animals during endotoxemia, indicating an essential role for the spleen in the cholinergic anti-inflammatory pathway. Furthermore, splenectomy reduces the production of antibodies directed against oxidized LDL in apoE-deficient mice and was associated with increased atherosclerotic lesion development (9). Trauma patients who undergo splenic removal are more prone to develop coronary heart disease, in which enhanced atherosclerotic lesion development may be causal (10).

Taken together, these findings suggests that autonomic innervation of the spleen and the development of atherosclerosis may be closely interrelated. Therefore, the aim of this study was to determine the effect of selective parasympathetic denervation (Px), as compared to sympathetic denervation (Sx) of the spleen and sham surgery, on systemic inflammation and atherosclerotic lesion development in female APOE*3-Leiden.CETP mice, a well-established mouse model for human-like lipoporotein metabolism.

Material and Methods

Animals

APOE*3-Leiden mice were crossbred with mice expressing human cholesteryl ester transfer protein (CETP) under control of its natural flanking regions to generate heterozygous APOE*3-Leiden.CETP mice (11). Mice were housed under standard conditions with a 12:12h light:dark cycle and had free access to food and water. At the age of 10-12 weeks, female APOE*3-Leiden.CETP mice received a Western-type diet (WTD) containing 0.1% cholesterol (w/w), 1% (w/) corn oil and 15% (w/w) cacao butter (AB diets, Woerden, the Netherlands). After a run-in period of 4 weeks, mice (n=45) were randomized based on plasma lipid levels and body weight into three groups (n=15 each) receiving either splenic parasympathetic denervation (Px), splenic sympathetic denervation (Sx) or sham surgery. A schematic representation of the innervation of the spleen and the sites of denervation can be found in **Figure 1A**. For all surgeries, mice were anesthetized by an intraperitoneal (i.p.) injection of a mixture of fentanylcitrate/fluanisone (Hypnorm; Janssen, Beerse, Belgium), midazolam (Dormicum; Roche, Mijdrecht, The Netherlands), and H_2O (1: 1: 2, v/v). All animal experiments had been approved by the Institutional Ethics Committee on Animal Care and Experimentation.

Selective parasympathetic denervation of the spleen

Since parasympathetic nerves enter the spleen at both tips, these tips were sequentially exposed during surgery to allow cutting of the nerves. After a midline abdominal incision the spleen was pulled gently towards the site of the incision, and the nerve at the tip of the spleen was cut. The connective tissue between the tip and the first hilus was also removed, as some parasympathetic input reaches the spleen via this connective tissue. Subsequently, the spleen was further pulled towards the midline to reach the lower tip of the spleen. After following back the nerve to the plexus, the connective tissue from this plexus back to the spleen was removed. The wound was closed with novosyn suture (B. Braun Medical, Oss, The Netherlands) (12).

Selective sympathetic denervation of the spleen

A midline abdominal incision was performed along the linea alba and the stomach was pushed up and to the right to reveal the blood vessels to and from the spleen. After the arterial branch to the stomach a bifurcation indicates the first branching point of the arterial supply to the spleen. From this bifurcation on the arteries will split many times and end at the hili of the spleen. Sympathetic nerves run along and around these arteries to reach the spleen. The area just before and after the bifurcation was chosen to remove the sympathetic nerves. The wound was closed

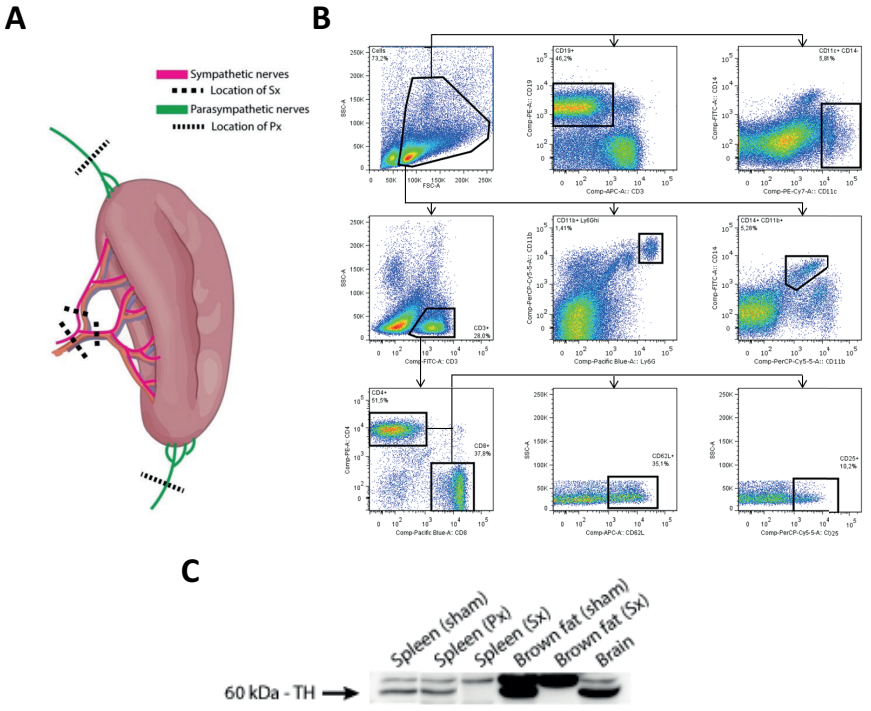

Figure 1 – Confirmation of splenic denervations and gating strategy. Schematic representation of the innervation of the spleen (**A**). The sympathetic input (pink) reaches the spleen via the arteries, the parasympathetic input (green) reaches the spleen via both tips of the spleen. The location at which denervations were performed are shown by the dashed lines. Gating strategy for flow cytometry analysis (**B**). Confirmation of sympathetic denervation (**C**) by measurement of tyrosine hydroxylase protein content of the spleen. As controls, TH content for the brain and (denervated) brown fat are included.

with novosyn suture (B. Braun Medical, Oss, The Netherlands) (12). Sympathetic denervation was confirmed 15 weeks after surgery by measurement of Tyrosine hydroxylase (TH) content Western blotting (anti-TH antibody; AB-112; Abcam).

Gene expression analysis in spleen, liver and peritoneal leukocytes

After surgery, the mice were fed the WTD for another 15 weeks. Subsequently, mice were sacrificed and organs were collected and peritoneal leukocytes isolated by lavage of the peritoneum with ice-cold PBS. Total RNA from spleen, liver and peritoneal leukocytes was isolated using the Nucleospin RNA II kit (Macherey-Nagel, Düren, Germany) according to manufacturer's instructions. One microgram of total RNA was converted to cDNA with iScript cDNA Synthesis kit (Biorad) and purified with Nucleospin Extract II kit (Macherey-Nagel). Real-time polymerase chain reaction

(RT-PCR) was conducted on the IQ5 PCR machine (Biorad) using the Sensimix SYBR Green RT-PCR mix (Quantace, London, UK). mRNA levels were normalized to mRNA levels of ß2 microglobulin, cyclophilin, and acidic ribosomal phosphoprotein P0 (36B4).

Flow cytometry analysis

From five randomly selected animals per group, peripheral blood and spleens were processed for flow cytometry. Thereto, single cell suspensions were obtained by mashing the cells trough a 70 µm cell strainer (Falcon, The Netherlands). Subsequently, cells were counted and $2x10^6$ cells were stained with appropriate antibodies (**Table 1**) to determine immune cell subsets: Live immune cells were selected from the forward and sideward scatter, and populations of B-cells (CD19+), dendritic cells (CD11c+CD14-), T-cells (CD3+), neutrophils (CD11b+Ly6Ghigh), and macrophages (CD14+CD11b+) were identified. Specific T cell subsets were determined within the CD3+ fraction as T helper cells (CD4+), cytotoxic T cells (CD8+), activated T cells (CD25+), naïve T cells (CD62L+). Data were acquired on a FACSAria or a FACSCanto II (BD Biosciences). Analyses were performed using FlowJo software (Treestar, Ashland, OR, USA). Gating strategy is shown in **Figure 1B**.

Table 1 – Detailed information of antibodies used for flow cytometry analysis

Antibody	Conjugate	Clone	Source	Dilution
CD19	PE	ID3	BD	1,600
CD14	FITC	Sa14-2	eBioscience	500
CD11c	Biotin	HL3	BD	200
CD3	APC	145-2C11	BD	300
CD3	FITC	145-2C11	BD	400
CD11b	PerCP	M1/70	BD	800
Ly6G	Ef450	RB6-8C5	eBioscience	800
CD4	PE	L3T4 GK1.5	BD	1,000
CD8	biotin	53-6.7	BD	400
CD62L	APC	MEL-14	Biolegend	1,600
CD25	PerCP	PC61	BD	500
Second step: Sav-PE-Cy7			BD	500

Serum measurements

Serum was isolated and stored frozen at -80°C until further analyses. The cytokines TNFα, IL-1ß and IL-6 were determined using V-PLEX Proinflammatory Panel1 (mouse) Kit (Meso Scale Discovery, Rockville, ML, USA) according to the manufacturer's instructions. In 50x diluted serum samples, E-selectin concentrations were measured according to the manufacturer's instructions (DY575, R&D systems, Minneapolis, MN, USA).

Plasma lipid and lipoprotein analyses

Blood was collected after a 4-h fast into EDTA-containing cups by tail bleeding, and plasma was isolated by centrifugation and stored frozen at -80°C until further analyses. The concentrations of total cholesterol (TC) and triglycerides (TG) in plasma were determined using commercially available enzymatic colorimetric kits according to the manufacturer's protocols (236691 and 1488872; Roche Molecular Biochemicals, Indianapolis, IN, USA). The concentrations of phospholipids (PL) in plasma were determined using a commercially available enzymatic colorimetric kit (3009; Instruchemie, Delfzijl, The Netherlands). The distribution of lipids over the different lipoproteins in plasma was determined after fractionation of pooled plasma (14-15 mice per pool) by FPLC using a Superose 6 HR 10/30 column (Äkta System; Amersham Pharmacia Biotech, Piscataway, NJ).

Atherosclerosis quantification

From all mice, hearts were isolated and fixed in phosphate-buffered 4% formaldehyde, dehydrated and embedded in paraffin. Cross-sections (5 μm) were made throughout the aortic root area and stained with hematoxylin-phloxine-saffron for histological analysis. Lesions were categorized for severity according to the guidelines of the American Heart Association adapted for mice (13). Various types of lesions were discerned: no lesions, mild lesions (types 1-3) and severe lesions (types 4-5). Immunohistochemistry for determination of lesion composition was performed as described previously (14). Rat anti-mouse antibody MAC3 (1:1000; BD Pharmingen, Breda, The Netherlands) was used to quantify macrophage area. Monoclonal mouse antibody M0851 (1:800; Dako, Heverlee, the Netherlands) against smooth muscle cell (SMC) α-actin was used to quantify SMC area. Sirius Red was used to quantify collagen area. Lesion area was quantified in the aortic root starting from the appearance of open aortic valve leaflets in four subsequent sections with 50 μm intervals. In ImageJ the lesions were delineated to determine mean lesion area (in μm^2) and a color threshold was set to determine the area percentage of MAC3, SMC or collagen staining in a consistent manner across the different slides.

Statistical analysis

Data are presented as means ± SEM unless indicated otherwise. To compare differences among groups one-way ANOVA with Turkey's post-test was performed using GraphPad Prism version 4.00 for Windows (GraphPad Software, San Diego, CA, USA, www.graphpad.com). Differences at a P-value <0.05 were considered statistically significant.

Results

Female APOE*3-Leiden.CETP mice were fed a WTD during 4 weeks, and were randomized into three groups receiving either parasympathetic denervation (Px) of the spleen, sympathetic denervation (Sx) of the spleen (**Figure 1A**), or sham surgery. After surgery, the mice received WTD feeding for 15 additional weeks to induce atherosclerotic lesion development. To confirm that Sx was successful and that sympathetic nerves did not regenerate, tyrosine hydroxylase (TH) content of the spleen was determined (**Figure 1C**), showing the absence of TH still 15 weeks after Sx. Upon sacrification of the mice, the tips of the spleen were gently exposed to confirm that the re-innervation of the parasympathetic nerves was not the case.

Splenic parasympathetic denervation increases immune cell count in spleen

The spleen plays an important role in the immune system and, therefore, contains a wide range of immune cell types, including monocytes, macrophages, dendritic cells, neutrophils, T cells and B cells. To define the effect of the selective denervations on immune cell composition, flow cytometry analyses were performed. Total splenic immune cell count was increased (+49%, $p<0.01$) in Px mice (200±10 $x10^6$ cells) compared to sham operated mice (134±10 $x10^6$ cells), while Sx denervation did not affect immune cell count (156±25 $x10^6$ cells) (**Figure 2A**). In a fraction of immune cells (i.e. 2.0$x10^6$ cells), percentages of each cell type were analyzed using flow cytometry and multiplied with total immune cell counts (see **Figure 1B** for the gating strategy). This revealed an increase in the number of various immune cell subtypes, including B cells (98±7 $x10^6$ cells *vs.* 61±5 $x10^6$ cells, $p<0.01$) (**Figure 2B**), T cells (63±4 $x10^6$ cells *vs.* 41±4 $x10^6$ cells, $p<0.01$) (**Figure 2C**) and dendritic cells (DCs; 10±1 $x10^6$ cells *vs.* 7±1 $x10^6$ cells, $p<0.05$) (**Figure 2D**). Neutrophils (**Figure 2E**) and monocytes/macrophages (**Figure 2F**) only showed a non-significant increase upon Px.

As T cells are integral to the cholinergic anti-inflammatory pathway (15), the phenotype of the T cells (i.e naivity or activation status of the T helper or cytotoxic T cells) was further studied. In accordance to the general increase in various immune cells, Px increased both T-helper (T_H; +60%, $p<0.01$) (**Figure 2G**) and cytotoxic T cells (T_{cyt}; +49%, $p<0.01$) (**Figure 2H**). Further subdivision revealed that Px increased naïve (**Figure 2I**) as well as activated (**Figure 2J**) T_H cells, and increased naïve T_{cyt} cells (**Figure 2K**) without increasing activated T_{cyt} cells (**Figure 2L**). Thus, splenic Px resulted in an overall increase in immune cells in the spleen, while Sx did not affect immune cell count compared to sham surgery, indicating the importance of the parasympathetic nerve in regulation of the immune system.

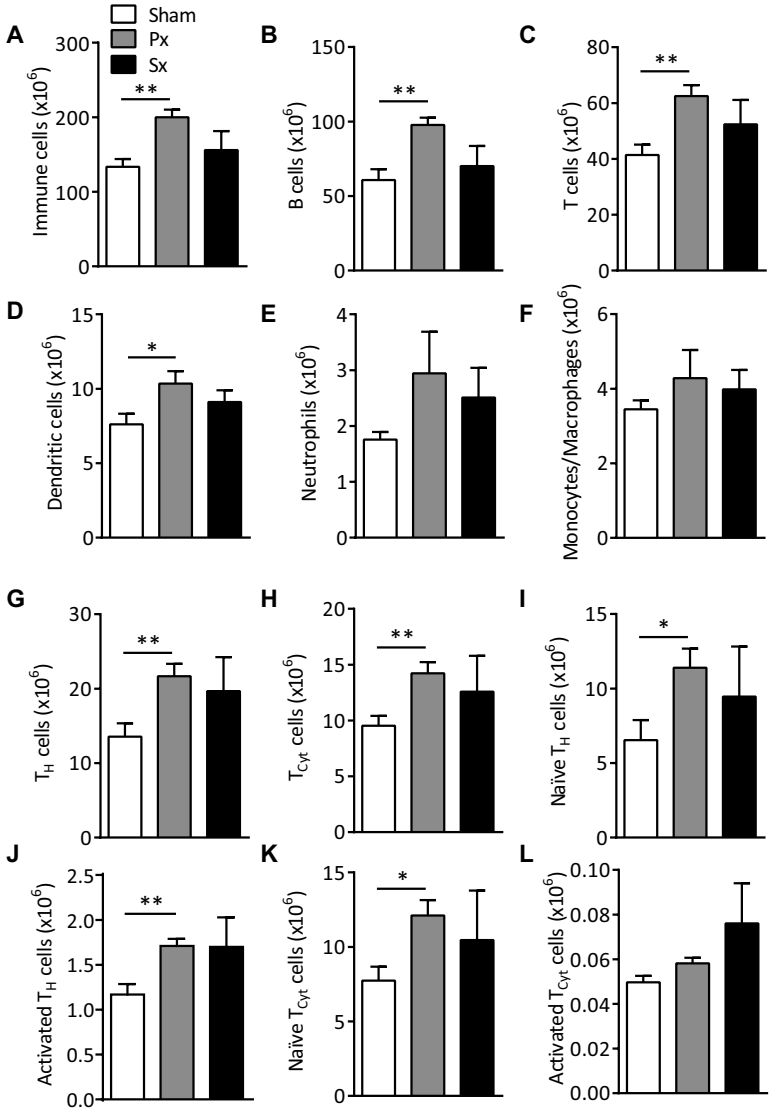

Figure 2 – Effect of splenic denervation on immune cell composition of the spleen. APOE*3-Leiden.CETP mice were fed a WTD during 4 weeks, were randomized into three groups receiving either splenic parasympathetic denervation (Px), sympathetic denervation (Sx), or sham surgery (t=0). Mice were fed a WTD during 15 additional weeks before spleens were isolated and cellular composition was analyzed by flow cytometry. Immune cells were counted based on FSC (**A**) and further subdivided into B-cells ($CD19^+$) (**B**), T-cells ($CD3^+$) (**C**), dendritic cells ($CD11c^+CD14^-$) (**D**), neutrophils ($CD11b^+Ly6G^{high}$) (**E**) and monocytes/macrophages ($CD14^+CD11b^+$) (**F**). Specific T cells subsets were identified as T_H (CD4+) (**G**), T_{Cyt} (CD8+) (**H**), naïve T_H (CD4+CD62L+) (**I**), activated T_H (CD4+ CD25+ (**J**), naïve T_{Cyt} (CD8+CD62L+) (**K**) and activated T_{Cyt} (CD8+ CD25+ (**L**). Values represent means ± SEM of 5 mice per group. *p<0.05, **p<0.01 compared to sham surgery.

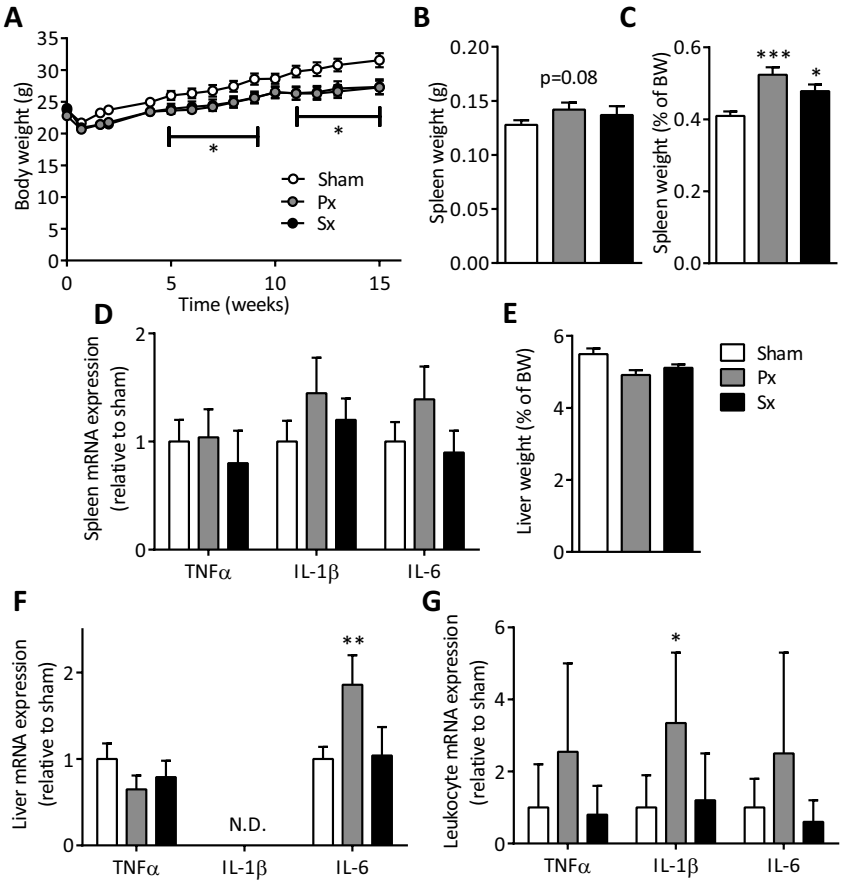

Figure 3 – Effect of splenic denervation on the gene expression of inflammatory genes. During the course of the experiment body weight was monitored (**A**). At 15 weeks after Px, Sx or sham surgery, spleens were weighed (**B**) and splenic weight was expressed as percentage of body weight (**C**), total RNA was extracted and expression levels of TNFα, IL-1β and IL-6 were determined by real-time PCR (**D**). Similarly, livers were weighed (**E**) and hepatic expression of these genes was determined (**F**). Peritoneal leukocytes were isolated and gene expression was quantified (**G**). Values represent means ± SEM of 15 mice per group *p<0.05, **p<0.01, ***p<0.01 compared to sham surgery.

Splenic parasympathetic denervation increases expression of inflammatory cytokines

During the course of the experiment, body weight gain was slightly lower in both Px and Sx mice. At the end of the experiment, body weight of sham operated mice was 31.6 ±1.1 g, compared to 27.3 ±1.1 g ($p<0.05$) and 27.4 ±1.2 g ($p<0.05$) for Px and Sx mice, respectively (**Figure 3A**). Splenic weight tended to be increased in Px (**Figure 3B**) and was different when expressed as percentage of the body weight for Px (0.52 ±0.02 %; $p<0.001$) and Sx (0.47 ±0.02 %; $p<0.05$) compared to sham (0.41 ±0.01 %) (**Figure 3C**). Gene expression analyses revealed that Px only caused a trend towards an increase of the inflammatory cytokines IL-1ß and IL-6 within the spleen (**Figure 3D**). Further analysis of other organs showed no difference in liver weight when expressed as percentage of the body weight (**Figure 3E**). Interestingly, Px increased gene expression of IL-6 in the liver (+80%; $p<0.01$) (**Figure 3F**) and increased gene expression of TNFα, IL-1ß and IL-6 in isolated peritoneal leukocytes, which reached significance for IL-1ß (3.3-fold; $p<0.05$) (**Figure 3G**). Next we determined the effect of Px on white blood cell count in peripheral blood and further analysed subsets by flow cytometry. Px tended to increase total immune cell count albeit significance was not reached (+41%; $p=0.18$) (**Figure 4A**). Subdivision of leukocytes into B cells (**Figure 4B**), T cells (**Figure 4C**), dendritic cells (**Figure 4D**), neutrophils (**Figure 4E**) or monocytes (**Figure 4F**) did not reveal differences. However, as the number of immune cells per se does not reflect activity of these cells, we measured serum levels of TNFα (**Figure 4G**), IL-1ß (**Figure 4H**) and IL-6 (**Figure 4I**) in serum. While TNFα levels remained unaffected, both IL-1ß and IL-6 serum concentrations were increased by Px. Interestingly, in contrast to our gene expression in liver, spleen and peritoneal leukocytes, also Sx increased inflammatory status as IL-1ß and IL-6 levels compared to sham operated mice.

Splenic parasympathetic denervation does not affect atherosclerotic lesion development

Since inflammation can influence lipid metabolism (16), we next evaluated whether selective splenic denervations had an effect on lipid metabolism. Plasma total cholesterol (TC), phospholipids (PL) and triglycerides (TG) were assessed at 2, 4, 6 and 15 weeks after surgery. No differences in plasma lipid concentrations were found between the Px, Sx and sham operated mice at weeks 2, 4, 6 (not shown) and 15 weeks (**Figure 4J**). Likewise, the distribution of cholesterol over the various lipoproteins did not differ between Px, Sx or sham control mice (**Figure 4K**). Serum E-selectin as marker for vascular inflammation, was increased in Px as well as in Sx compared to sham, suggesting that immune cell infiltration into atherosclerotic lesions might be enhanced by the selective denervations (**Figure 4L**).

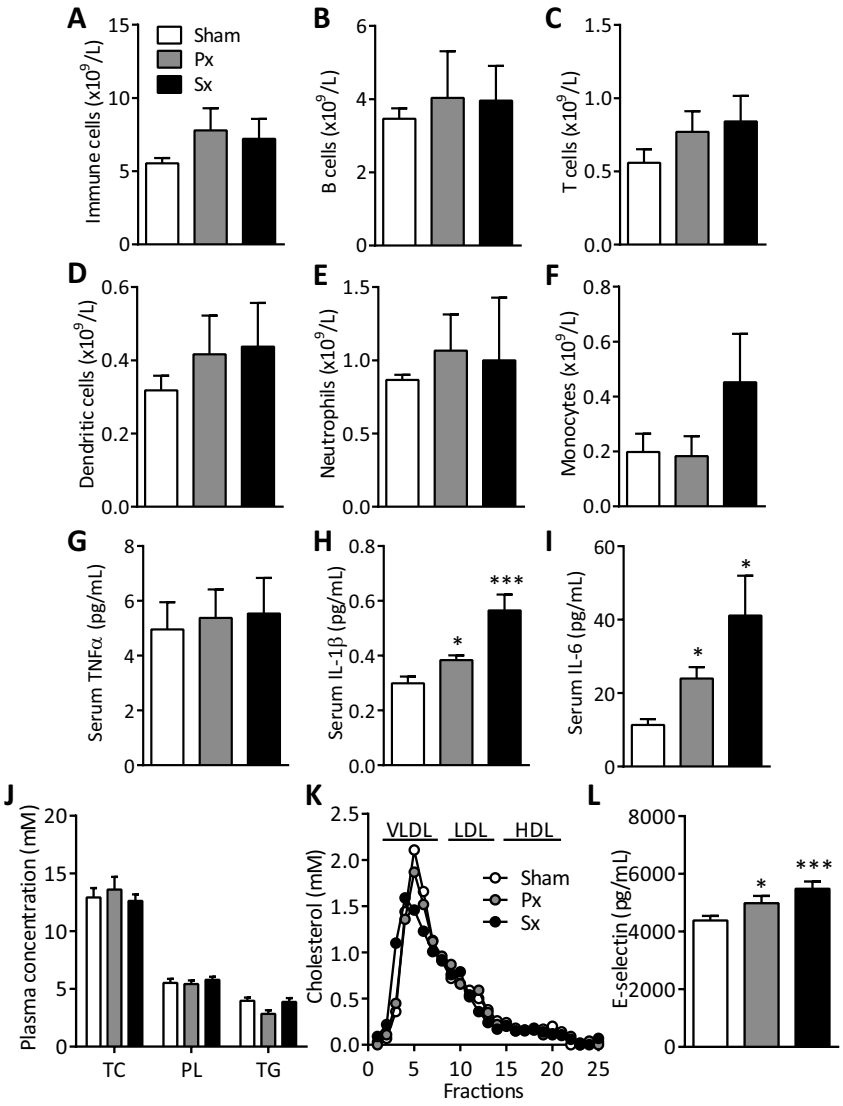

Figure 4 – Effect of splenic denervation on white blood cell composition, serum cytokines and plasma lipids. At 15 weeks after Px, Sx or sham surgery, blood was drawn and analyzed by flow cytometry. Immune cells were counted (**A**) and further subdivided into B-cells ($CD19^+$) (**B**), T-cells ($CD3^+$) (**C**), dendritic cells ($CD11c^+CD14^-$) (**D**), neutrophils ($CD11b^+Ly6G^{high}$) (**E**) and monocytes ($CD14^+CD11b^+$) (**F**). Serum cytokine levels of TNFα (**G**), IL-1β (**H**) and IL-6 (**I**) were measured. Plasma concentrations of total cholesterol (TC), phospholipids (PL) and triglycerides (TG) were determined (**J**). The distribution of cholesterol over the different lipoproteins was determined by fractionation of pooled plasma by FPLC (**K**). Serum E-selectin (**L**). Values represent means ± SEM of 5 (**A-F**) or 15 (**G-L**) mice per group.

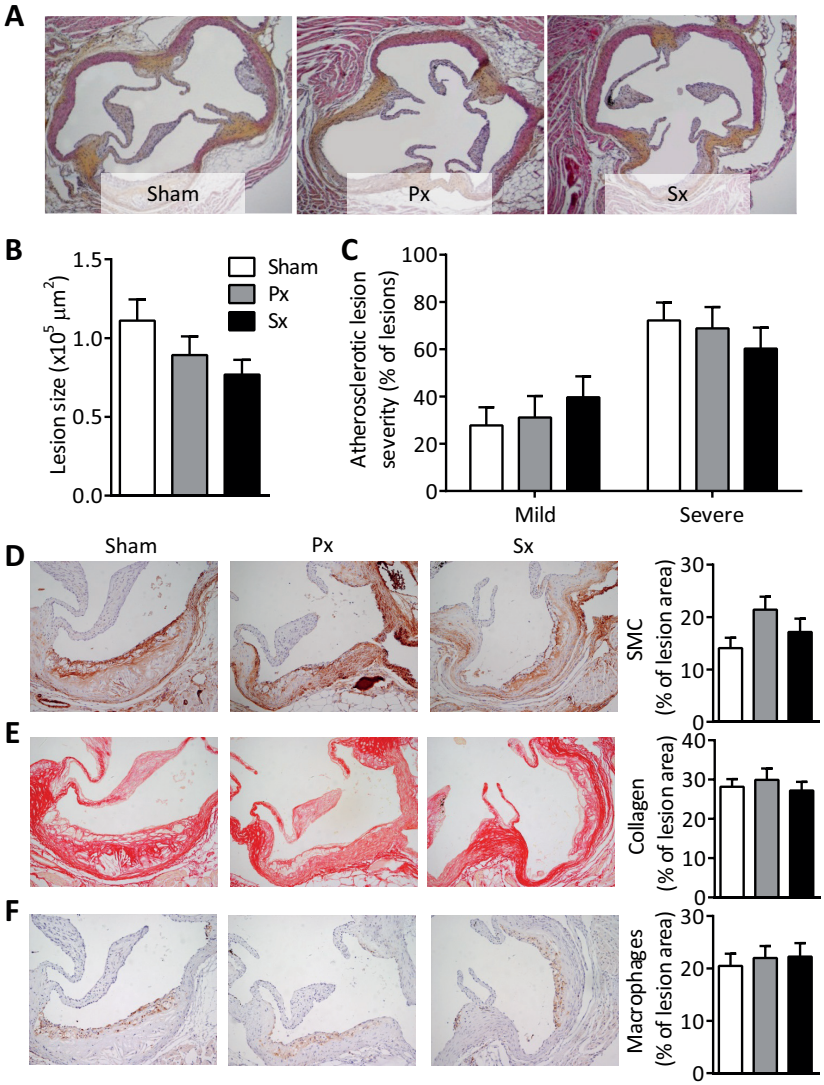

Figure 5 – Effect of splenic denervation on atherosclerotic lesion size and composition. At 15 weeks after Px, Sx or sham surgery, hearts were isolated and cross-sections (5 µm) with 50 µm intervals throughout the aortic root area starting from the appearance of open aortic valve leaflets were used for atherosclerosis measurements. Sections were stained with hematoxylin-phloxine-saffron for histological analysis and representative images are shown (**A**). Atherosclerotic mean lesion area (in µm^2) was quantified in four subsequent cross-sections (**B**). The same four sections per mouse were categorized according to lesion severity (**C**). Lesion composition was determined by immunohistochemistry in four subsequent cross-sections using α-actin for smooth muscle cells (SMC) (**D**), Sirius Red staining for collagen content (**E**) and MAC3 for macrophages (**F**). Values represent means ± SEM of 15 mice per group.

To study the effect of splenic denervation on atherosclerosis development, mice were sacrificed after 15 weeks after surgery, and atherosclerotic lesion size and lesion severity were determined in the valve area of the aortic root. Both Px and Sx did neither affect atherosclerotic lesion size (**Figure 5A,B**) nor lesion severity, when classified as mild (type 1-3) and severe (type 4-5) lesions (**Figure 5C**). However, also no significant differences were observed in lesion composition between Px, Sx and sham operated mice, with respect to the relative area of smooth muscle cells (SMC; α-actin staining; **Figure 5D**), collagen (Sirius Red staining; **Figure 5E**) and macrophages (MAC3 staining; **Figure 5F**).

Discussion

In the current study, we tested the hypothesis that the brain plays a prominent role in modulating the activity of immune cells and may therefore affect atherosclerosis development. We determined the effect of selective splenic parasympathetic denervation (Px), sympathetic denervation (Sx) on the inflammatory status and examined the potential consequences for plasma lipids and the development of atherosclerosis in APOE*3-Leiden.CETP mice. We showed that predominantly splenic Px increased the inflammatory state of the body as indicated by increased leukocyte counts within the spleen and increased pro-inflammatory cytokine expression. However, splenic Px as well as Sx did not affect atherosclerotic lesion development.

Interestingly, we found increased circulating levels of the pro-inflammatory cytokines IL-1ß and IL-6 upon both Px and Sx. Classically, the parasympathetic and sympathetic nerves system act in opposite direction to facilitate control over physiological responses to maintain homeostasis. However, for the spleen, it has been suggested that both systems in fact act together to restrain inflammation by projection of the vagus nerve also onto the sympathetic splenic nerve (6,17). Previous studies even suggested absence of direct parasympathetic innervation of the spleen as neither choline acetyltransferase nor vesicular acetylcholine transporter producing nerve endings could be detected within the spleen (6,18). However the absence of the classical vagus transmitter acetylcholine is not sufficient proof for the absence of direct input from the vagus. In previous studies we identified neuronal connections between the spleen and both the intermedio lateral column of the spinal cord (IML) and the dorsal motor nucleus of the vagus nerve (DMV) by retrograde tracing using pseudorabies virus (PRV) and cholera toxin-b (CTB) (12,19), suggesting sympathetic as well as parasympathetic neuronal connectivity. Surgical ablation of the nerves along the splenic arteries (similar to Sx) resulted in undetectable retrograde tracer in the IML and absence of TH in the spleen. In contrast, surgical ablation of the nerve branches at the splenic ends (similar to Px) resulted in a loss

of detectability of the tracers in the DMV and can therefore most likely be allocated to the parasympathetic nerves system. In addition, Px severely diminished (-70%) LPS-induced antibody production, clearly indicating functional involvement of these nerve branches in the control of the immune response (12). In contrast, Sx did not affect the production of specific antibodies. While absence of sympathetic input 15 wk after Sx was confirmed by measuring TH content, confirmation of Px was limited to visual inspection due to the lack of specific markers for these neurons. However, consistent with the notion that vagal activation suppresses the immune response (5), we found that Px enhances the number of leukocytes and increases expression of proinflammatory cytokines. It may seem contradictive that Px results in diminished LPS-induced antibody production (12), while here we report enhanced inflammatory responses. However, one should consider the dual challenge for the brain during inflammation, namely to contain the inflammation by for example reducing cytokine production and subsequently to induce memory within the immune system to prevent new infections by inducing antibody production.

Despite that Px increased the number of immune cells in the spleen in the current study, no differences in splenic TNFα gene expression or circulating TNFα were found. Possibly stronger inflammatory stimuli are required to attenuate TNFα production by spleen macrophages via stimulation of the vagus nerve, as has been shown for LPS-induced endotoxemia (6). Compatible with the notion that TNFα is crucially involved in the pathogenesis and progression of atherosclerosis (20,21), Px and Sx did not aggravate WTD-induced atherosclerotic lesion development and did not affect lesion composition in APOE*3-Leiden.CETP mice. Similarly, we previously showed that hematopoietic α7nAChR deficiency in $ApoE^{-/-}$ mice does increase inflammatory status of the body and enhances platelet reactivity, but does not aggravate atherosclerosis as lesion size and plaque composition remained unaffected (7). In contrast, Johansson *et al.* (22) recently reported an increase in atherosclerotic lesion development upon hematopoietic α7nAChR deficiency in $Ldlr^{-/-}$ mice, indicating that the genetic and environmental context are important to determine the outcome of disrupted anti-inflammatory reflexes. Despite conflicting outcomes, interfering with inflammatory reflexes might be an interesting target in the prevention of atherosclerosis. Several animal studies report beneficial effects of low dose ß-blockers on atherogenesis (23,24), mainly via reducing of inflammatory responses rather than changes in lipid metabolism. Also in humans, the use of metoprolol slows progression of intima-media thickness (25,26).

While the role of the autonomic splenic nerves in human physiology is unclear, splenectomy in trauma patients has been associated with frequency of ischemic coronary diseases, probably explained by increased plasma lipids (10). Rodent studies confirmed the role of the spleen in lipid metabolism as splenectomized rats showed reduced HDL-cholesterol and increased plasma triglycerides. Complete

removal of the spleen in ApoE-deficient mice increased plaque development, although the underlying mechanism remained elusive (9). In the current study, no differences in plasma lipids were found upon splenic denervations, suggesting that regulation of lipid metabolism via the spleen is probably not mediated via innervation of the splenic nerves, which may explain why atherosclerosis development was not aggravated in this study. Interestingly, splenectomized trauma patients do display increased infection rates and have increased leukocyte counts (27), corresponding with the data presented in the current study, however the exact contribution of an isolated increased inflammatory status without effects on plasma lipid levels to atherosclerosis development is unclear.

In conclusion, selective disruption of mainly the splenic parasympathetic nerve increases splenic immune cell counts and the systemic inflammatory status, but does not contribute to atherosclerotic lesion development.

Acknowledgements

P.C.N. Rensen is an Established Investigator of the Netherlands Heart Foundation (grant 2009T038).

References

1. Hansson, G. K. & Libby, P. (2006) The immune response in atherosclerosis: a double-edged sword. *Nat Rev Immunol* 6, 508-519.
2. Janig, W. (2014) Sympathetic nervous system and inflammation: a conceptual view. *Auton Neurosci* 182, 4-14.
3. Borovikova, L. V., Ivanova, S., Zhang, M. *et al.* (2000) Vagus nerve stimulation attenuates the systemic inflammatory response to endotoxin. *Nature* 405, 458-462.
4. Gallowitsch-Puerta, M. & Pavlov, V. A. (2007) Neuro-immune interactions via the cholinergic anti-inflammatory pathway. *Life Sci* 80, 2325-2329.
5. Wang, H., Yu, M., Ochani, M. *et al.* (2003) Nicotinic acetylcholine receptor alpha7 subunit is an essential regulator of inflammation. *Nature* 421, 384-388.
6. Rosas-Ballina, M., Ochani, M., Parrish, W. R. *et al.* (2008) Splenic nerve is required for cholinergic antiinflammatory pathway control of TNF in endotoxemia. *Proc Natl Acad Sci USA* 105, 11008-11013.
7. Kooijman, S., Meurs, I., van der Stoep, M. *et al.* (2014) Hematopoietic alpha7 nicotinic acetylcholine receptor deficiency increases inflammation and platelet activation status, but does not aggravate atherosclerosis. *J Thromb Haemost*
8. Huston, J. M., Ochani, M., Rosas-Ballina, M. *et al.* (2006) Splenectomy inactivates the cholinergic antiinflammatory pathway during lethal endotoxemia and polymicrobial sepsis. *J Exp Med* 203, 1623-1628.
9. Rezende, A. B., Neto, N. N., Fernandes, L. R. *et al.* (2011) Splenectomy increases atherosclerotic lesions in apolipoprotein E deficient mice. *J Surg Res* 171, e231-e236.
10. Robinette, C. D. & Fraumeni, J. F., Jr. (1977) Splenectomy and subsequent mortality in veterans of the 1939-45 war. *Lancet* 2, 127-129.
11. Westerterp, M., van der Hoogt, C. C., de, H. W. *et al.* (2006) Cholesteryl ester transfer protein decreases high-density lipoprotein and severely aggravates atherosclerosis in APOE*3-Leiden mice. *Arterioscler Thromb Vasc Biol* 26, 2552-2559.
12. Buijs, R. M., van, d., V, Garidou, M. L. *et al.* (2008) Spleen vagal denervation inhibits the production of antibodies to circulating antigens. *PLoS One* 3, e3152.
13. Wong, M. C., van Diepen, J. A., Hu, L. *et al.* (2012) Hepatocyte-specific IKKbeta expression aggravates atherosclerosis development in APOE*3-Leiden mice. *Atherosclerosis* 220, 362-368.
14. Hu, L., Boesten, L. S., May, P. *et al.* (2006) Macrophage low-density lipoprotein receptor-related protein deficiency enhances atherosclerosis in ApoE/LDLR double knockout mice. *Arterioscler Thromb Vasc Biol* 26, 2710-2715.
15. Rosas-Ballina, M., Olofsson, P. S., Ochani, M. *et al.* (2011) Acetylcholine-synthesizing T cells relay neural signals in a vagus nerve circuit. *Science* 334, 98-101.
16. van Diepen, J. A., Berbee, J. F., Havekes, L. M. *et al.* (2013) Interactions between inflammation and lipid metabolism: relevance for efficacy of anti-inflammatory drugs in the treatment of atherosclerosis. *Atherosclerosis* 228, 306-315.
17. Vida, G., Pena, G., Deitch, E. A. *et al.* (2011) alpha7-cholinergic receptor mediates vagal induction of splenic norepinephrine. *J Immunol* 186, 4340-4346.
18. Berthoud, H. R. & Powley, T. L. (1996) Interaction between parasympathetic and sympathetic nerves in prevertebral ganglia: morphological evidence for vagal efferent innervation of ganglion cells in the rat. *Microsc Res Tech* 35, 80-86.
19. Cailotto, C., Costes, L. M., van, d., V *et al.* (2012) Neuroanatomical evidence demonstrating the existence of the vagal anti-inflammatory reflex in the intestine. *Neurogastroenterol Motil* 24, 191-200, e93.
20. Branen, L., Hovgaard, L., Nitulescu, M. *et al.* (2004) Inhibition of tumor necrosis factor-alpha reduces atherosclerosis in apolipoprotein E knockout mice. *Arterioscler Thromb Vasc Biol* 24, 2137-2142.
21. Kleinbongard, P., Heusch, G., & Schulz, R. (2010) TNFalpha in atherosclerosis, myocardial ischemia/reperfusion and heart failure. *Pharmacol Ther* 127, 295-314.

22. Johansson, M. E., Ulleryd, M. A., Bernardi, A. *et al.* (2014) alpha7 Nicotinic acetylcholine receptor is expressed in human atherosclerosis and inhibits disease in mice--brief report. *Arterioscler Thromb Vasc Biol* 34, 2632-2636.
23. Shimada, K., Hirano, E., Kimura, T. *et al.* (2012) Carvedilol reduces the severity of atherosclerosis in apolipoprotein E-deficient mice via reducing superoxide production. *Exp Biol Med (Maywood)* 237, 1039-1044.
24. Ulleryd, M. A., Bernberg, E., Yang, L. J. *et al.* (2014) Metoprolol reduces proinflammatory cytokines and atherosclerosis in ApoE-/- mice. *Biomed Res Int* 2014, 548783.
25. Hedblad, B., Wikstrand, J., Janzon, L. *et al.* (2001) Low-dose metoprolol CR/XL and fluvastatin slow progression of carotid intima-media thickness: Main results from the Beta-Blocker Cholesterol-Lowering Asymptomatic Plaque Study (BCAPS). *Circulation* 103, 1721-1726.
26. Wiklund, O., Hulthe, J., Wikstrand, J. *et al.* (2002) Effect of controlled release/extended release metoprolol on carotid intima-media thickness in patients with hypercholesterolemia: a 3-year randomized study. *Stroke* 33, 572-577.
27. (1996) Guidelines for the prevention and treatment of infection in patients with an absent or dysfunctional spleen. *BMJ* 312, 430-434.